Astronomy & Astrophysics manuscript no. paper
February 9, 2012
© ESO 2012

arXiv:1202.1455v2 [astro-ph.GA] 8 Feb 2012

Implications on the X-ray emission of evolved pulsar wind nebulae based on VHE γ-ray observations

M. Mayer[1,2], J. Brucker[1], I. Jung[1], K. Valerius[1], and C. Stegmann[2,3,4]

[1] Erlangen Centre for Astroparticle Physics (ECAP), Universität Erlangen-Nürnberg, Erwin-Rommel-Str. 1, D-91058 Erlangen, Germany
[2] Institut für Physik und Astronomie, Universität Potsdam, Karl-Liebknecht-Str. 24/25, D-14476 Potsdam-Golm, Germany
[3] DESY, Platanenallee 6, D-15738 Zeuthen, Germany
[4] Formerly at [1]

Received 7 February 2012 / Accepted

ABSTRACT

Context. Energetic pulsars power winds of relativistic leptons which produce photon nebulae (so-called pulsar wind nebulae, PWNe) detectable across the electromagnetic spectrum up to energies of several TeV. The spectral energy distribution has a double-humped structure: the first hump lies in the X-ray regime, the second in the γ-ray range. The X-ray emission is generally understood as synchrotron radiation by highly energetic electrons, the γ-ray emission as Inverse Compton scattering of energetic electrons with ambient photon fields. The evolution of the spectral energy distribution is influenced by the time-dependent spin-down of the pulsar and the decrease of the magnetic field strength with time. Thus, the present spectral appearance of a PWN depends on the age of the pulsar: while young PWNe are bright in X-rays and γ-rays, the X-ray emission of evolved PWNe is suppressed. Hence, evolved pulsar wind nebulae may offer an explanation of the nature of some of the unidentified VHE γ-ray sources not yet associated with a counterpart in other high-energy ranges.
Aims. The purpose of this work is to develop a model which allows to calculate the expected X-ray fluxes of unidentified VHE γ-ray sources considered to be PWN candidates. Such an estimate helps to evaluate the prospects of detecting the X-ray signal in deep observations with current X-ray observatories in future studies.
Methods. We present a time-dependent leptonic model which predicts the broad-band emission of a PWN according to the characteristics of its pulsar. The values of the free parameters of the model are determined by a fit to observational VHE γ-ray data. For a sample of representative PWNe, the resulting model predictions in the X-ray and γ-ray range are compared to observations.
Results. The comparison shows that the high-energy emission of identified PWNe from different states of evolution is predicted correctly by the model.

Key words. Pulsars: general; Gamma rays: general; ISM: supernova remnants; ISM: individual objects: (MSH 15−5*2*; HESS J1825−137; HESS J1837−069); Radiation mechanisms: non-thermal;

1. Introduction

During the last decade, a new generation of Imaging Atmospheric Cherenkov Telescopes (IACTs) has discovered an increasing number of Galactic sources emitting VHE (very high energy, $E > 100\,\mathrm{GeV}$) γ-rays. Among these, pulsar wind nebulae (PWNe) form the most abundant class. Such nebulae are usually associated with the non-thermal emission from a magnetized plasma of relativistic particles fed by an energetic pulsar. In current models, the plasma is thought to consist mainly of energetic leptons (see e.g. Gaensler & Slane, 2006) which emit non-thermal radiation over a wide energy range. Interacting with magnetic fields, the leptons produce synchrotron radiation up to several keV. In addition, low-energy photons, e.g. from the cosmic microwave background (CMB), can be up-scattered by the energetic leptons to very high energies via the Inverse Compton effect. Therefore, the emission in X-rays and VHE γ-rays is tightly linked, emerging from the same lepton population (see, e.g. Gelfand et al., 2009).
The second largest population of Galactic VHE γ-ray sources consists of unidentified sources without an unambigious counterpart at other wavelengths (see, e.g., Aharonian et al., 2008). However, in many cases an energetic pulsar can be found in the vicinity, suggesting a possible connection between these unidentified objects and pulsar wind nebulae. Provided that the rotational period and its first time derivative can be measured, e.g. by radio observations, the spin-down energy loss of the pulsar can be estimated and hence the viability of the pulsar as an energy source of the nebula can be investigated. In addition, in the PWN scenario of broad-band emission by energetic leptons a spatial association of the VHE γ-ray source with an X-ray nebula counterpart is expected. There are mainly two issues complicating this identification scheme: In some cases, PWNe are slightly displaced from the pulsar, which may result from an interaction with the supernova remnant reverse shock (see, e.g., Blondin et al., 2001) and from a

Send offprint requests to: M. Mayer, e-mail: michael.mayer@desy.de

proper motion of the pulsar, gained from a kick at its birth (e.g. van der Swaluw et al., 2004). Furthermore, in particular for older systems the X-ray emission becomes harder to detect since the energetic leptons injected in earlier epochs have been cooled and, at the same time, the supply of fresh leptons is reduced. Moreover, the synchrotron emission by the freshly injected leptons is suppressed because the magnetic field strength decreases with time. Since the accumulated less energetic leptons can still produce VHE γ-rays via Inverse Compton (IC) scattering, such evolved PWNe have been proposed (e.g. de Jager & Djannati-Ataï, 2009) as an explanation of some of the as yet unidentified VHE γ-ray sources.

In this work we introduce a time-dependent leptonic model of the non-thermal emission of PWNe (Section 2) and apply the model to PWNe of different evolutionary states (Section 3). For each individual source, the free parameters are fixed by fitting the model to the VHE γ-ray data. Subsequently, we show that the X-ray emission of these objects is predicted correctly by the fitted model. Hence, in future studies it may serve as a means to estimate the X-ray flux of unidentified VHE γ-ray sources in a PWN scenario, allowing to evaluate the prospects of detection in deep observations with current X-ray observatories.

2. The Model

In this Section we introduce a leptonic model describing the time evolution of the non-thermal radiation from PWNe. The time dependence of the energy output $\dot{E}$ of the pulsar, which derives from the slow-down of the rotation, has to be taken into account:

$$\dot{E} = -\frac{\mathrm{d}E_{\mathrm{rot}}}{\mathrm{d}t}. \tag{1}$$

Following Pacini & Salvati (1973), the energy output evolves with time as

$$\dot{E}(t) = \dot{E}_0 \left(1 + \frac{t}{\tau_0}\right)^{-\frac{n+1}{n-1}}, \tag{2}$$

where $\dot{E}_0 = \dot{E}(t=0)$, τ_0 denotes the spin-down timescale of the pulsar and n the braking index. The latter has been measured only for a few young pulsars (Camilo et al., 2000, and references therein). Such a measurement exists, for instance for PSR B1509−58, which is one of the sample pulsars discussed in Section 3. Thus, for the modeling of the PWN associated with PSR B1509−58 we used the measured value of $n = 2.839$ (Livingstone et al., 2005). For the other cases we adopted $n = 3$ (Manchester & Taylor, 1977), corresponding to spin-down via magnetic dipole radiation. The spin-down timescale τ_0 is defined by

$$\tau_0 = \frac{2\tau_{\mathrm{c}}}{n-1}\left(\frac{P_0}{P}\right)^{n-1}, \tag{3}$$

with P_0 and P being the initial and the current period, respectively, and $\tau_{\mathrm{c}} = P/(2\dot{P})$ the characteristic age of the pulsar ($\dot{P}$ denoting the time derivative of the rotational period). For $n = 3$ and $P_0 \ll P$ the present true age T of the pulsar corresponds to the characteristic age τ_{c}, whereas for other cases it can be calculated as

$$T = \frac{P}{(n-1)\dot{P}}\left(1 - \left(\frac{P_0}{P}\right)^{n-1}\right). \tag{4}$$

P and $\dot{P}$ can usually be derived from radio observations, while the initial period will be treated as a free parameter of our model.

In the following, the evolution of the non-thermal emission of a PWN is calculated in discrete time steps with an adaptive step size of δt. In each time step only a fractional amount ΔE_{p} of the energy output of the pulsar is converted into relativistic leptons, i.e. electrons and positrons. Assuming the corresponding conversion efficiency η to be constant over time, $\Delta E_{\mathrm{p}}(t)$ is determined as

$$\Delta E_{\mathrm{p}}(t) = \eta \int_t^{t+\delta t} \dot{E}(t')\mathrm{d}t' \tag{5}$$

for a time interval $[t, t+\delta t]$ and with $\eta \in [0;1]$. The conversion efficiency is strongly correlated with P_0, such that the quality of the fit does not benefit from an additional free parameter. Therefore η is fixed to the value of 0.3, which is in agreement with e.g. the modeling results for MSH 15−5*2* carried out by Schöck et al. (2010) and Zhang et al. (2008). We assume that the differential energy spectrum of the injected leptons can be described by a simple power law

$$\frac{\mathrm{d}N_{\mathrm{inj}}}{\mathrm{d}E}(E,t) = \Phi_0(t)\left(\frac{E}{1\,\mathrm{TeV}}\right)^{-2}. \tag{6}$$

Assuming that the spectral shape does not change within a time bin, $\Phi_0(t)$, denoting the normalization of the distribution at 1 TeV, can be calculated by integrating the injection spectrum over energy:

$$\Delta E_{\mathrm{p}}(t) \stackrel{!}{=} \int_{E_{\mathrm{min}}}^{E_{\mathrm{max}}} \frac{\mathrm{d}N_{\mathrm{inj}}}{\mathrm{d}E}(E,t)\,\mathrm{d}E\,. \tag{7}$$

We only consider leptons injected into the pulsar wind in the range between $E_{\mathrm{min}} = 0.1\,\mathrm{TeV}$ and $E_{\mathrm{max}} = 1000\,\mathrm{TeV}$, well suited to accomodate the VHE γ-rays as well as the X-ray emission from PWNe. Leptons with energies outside this range do not significantly contribute to the emission in the considered photon wavebands. Given a differential yield of leptons $\mathrm{d}N(E, t-\delta t)/\mathrm{d}E$ with energy E at a time $t - \delta t$ the number of leptons remaining after cooling at the time t can be calculated. Following Zhang et al. (2008), the cooling of the lepton population during a time step δt is implemented in the model by an exponential function:

$$\frac{\mathrm{d}N_{\mathrm{cooled}}}{\mathrm{d}E}(E,t) = \frac{\mathrm{d}N}{\mathrm{d}E}(E, t-\delta t)\cdot\exp\left(-\frac{\delta t}{\tau_{\mathrm{eff}}(E,t)}\right). \tag{8}$$

This approach uses an effective cooling time scale $\tau_{\mathrm{eff}}^{-1} = \tau_{\mathrm{syn}}^{-1} + \tau_{\mathrm{esc}}^{-1}$ taking into account both synchrotron and escape losses. The respective time scales τ_{syn} and τ_{esc} are likewise adopted from Zhang et al. (2008):

$$\tau_{\mathrm{syn}}(E,t) = 12.5\cdot\left[\frac{B(t)}{10\,\mu\mathrm{G}}\right]^{-2}\cdot\left[\frac{E}{10\,\mathrm{TeV}}\right]^{-1}\mathrm{kyr} \tag{9}$$

$$\tau_{\mathrm{esc}}(E,t) = 34\cdot\left[\frac{B(t)}{10\,\mu\mathrm{G}}\right]\cdot\left[\frac{E}{10\,\mathrm{TeV}}\right]^{-1}\cdot\left[\frac{R(t)}{1\,\mathrm{pc}}\right]^{2}\mathrm{kyr}, \tag{10}$$

where $R(t)$ and $B(t)$ describe the time evolution of the PWN radius and the magnetic field strength inside the PWN, respectively. For evolved PWNe, $R(t)$ is given by (see Gaensler & Slane, 2006, and references therein):

$$R(t) = \begin{cases} a\cdot t^{11/15} & \text{for} \quad t < \tau_0 \\ b\cdot t^{3/10} & \text{for} \quad t \geq \tau_0 \end{cases}, \tag{11}$$

where the coefficients a and b can be calculated using the present-day size of the PWN. Likewise, we assume that the radial extent of each freshly injected lepton population can be described by Eq. 11, where the age of the PWN is replaced by the corresponding age of the leptons. This approximation leads to an onion-like structure of the PWN model.

The magnetic field strength $B(t)$ is adapted from Zhang et al. (2008):

$$B(t) = \frac{B_0}{1 + (t/\tau_0)^\alpha} + B_{\rm ISM}\,. \quad (12)$$

$B_{\rm ISM}$ represents a time-independent component of $3\,\mu$G to account for the magnetic field strength of the ambient medium. The parameter α is fixed to a value of 0.5, which was also found in the studies of Zhang et al. (2008) and Qiao et al. (2009) for five PWNe (among them MSH 15−52 and HESS J1825−137 which are investigated in this work). Finally, B_0, the initial magnetic field strength inside the PWN, is a free parameter. All in all, the model has two free parameters (P_0 and B_0) defining the starting conditions of the PWN evolution.

Having established the framework for cooling and injection processes, we can calculate the number of leptons with energy E present in the nebula at a time $t + \delta t$. This number comprises leptons injected and cooled until time t as well as freshly injected leptons between t and $t + \delta t$:

$$\frac{{\rm d}N}{{\rm d}E}(E, t+\delta t) = \frac{{\rm d}N_{\rm cooled}}{{\rm d}E}(E,t) + \frac{{\rm d}N_{\rm inj}}{{\rm d}E}(E, t+\delta t). \quad (13)$$

By iteratively evaluating Eq. 13, it is possible to determine the energy distribution of the leptons inside the PWN at an arbitrary time. Based on this distribution, the corresponding photon population can be calculated, with synchrotron radiation and IC scattering as the most relevant emission processes in the considered energy range[1]. A detailed account of these mechanisms can be found in Blumenthal & Gould (1970). The target photon fields considered for IC scattering – CMB, starlight and infrared photons – are adopted from the GALPROP code (Porter & Strong, 2005).

As a first step, we can use the model to study the development of the spectral energy distribution (SED) with progressing age for a generic PWN system. The SED shown in Fig. 1 is based on the characteristics of the pulsar PSR J1826−1334 and its nebula (see Table 1), representing an example of an evolved PWN. The free parameters are exemplarily set to $P_0 = 30\,$ms and $B_0 = 50\,\mu$G.

Since the magnetic field strength decays strongly with time, the X-ray emission is suppressed for high PWN ages. At the same time energy-dependent cooling effects become visible in the γ-ray band, reducing the emissions in the VHE γ-ray range and shifting the peak to lower energies.

As a second application of the model, we investigate the contribution of leptons from different injection epochs to the current photon SED, as shown in Fig. 2 for our generic PWN. Summing up the SEDs from leptons of all epochs results in the emission visible today. The modeling shows

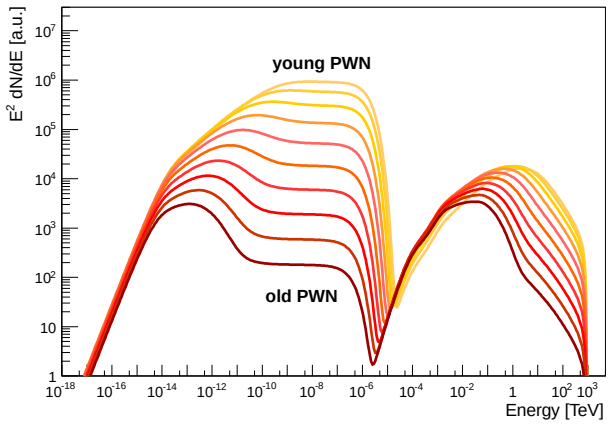


Fig. 1. Typical evolution of the modeled spectral energy distribution of a PWN with time. The color scale represents the age of the PWN, starting with a young system (500 years, yellow) and proceeding in equidistant steps on a logarithmic time scale to an old system (200 kyr, dark red).

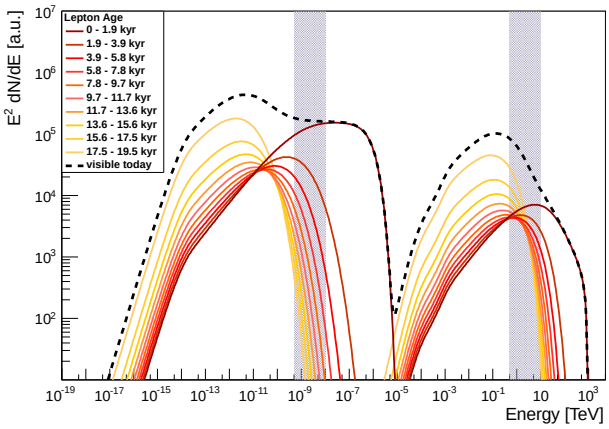


Fig. 2. Photon SED (black broken line) of a generic middle-aged (approximately 20 kyr) PWN decomposed into contributions by leptons from different injection epochs (solid colored lines). The same parameters as in Fig. 1 were used for this example.The grey areas represent the energy ranges covered by current X-ray and VHE γ-ray observatories.

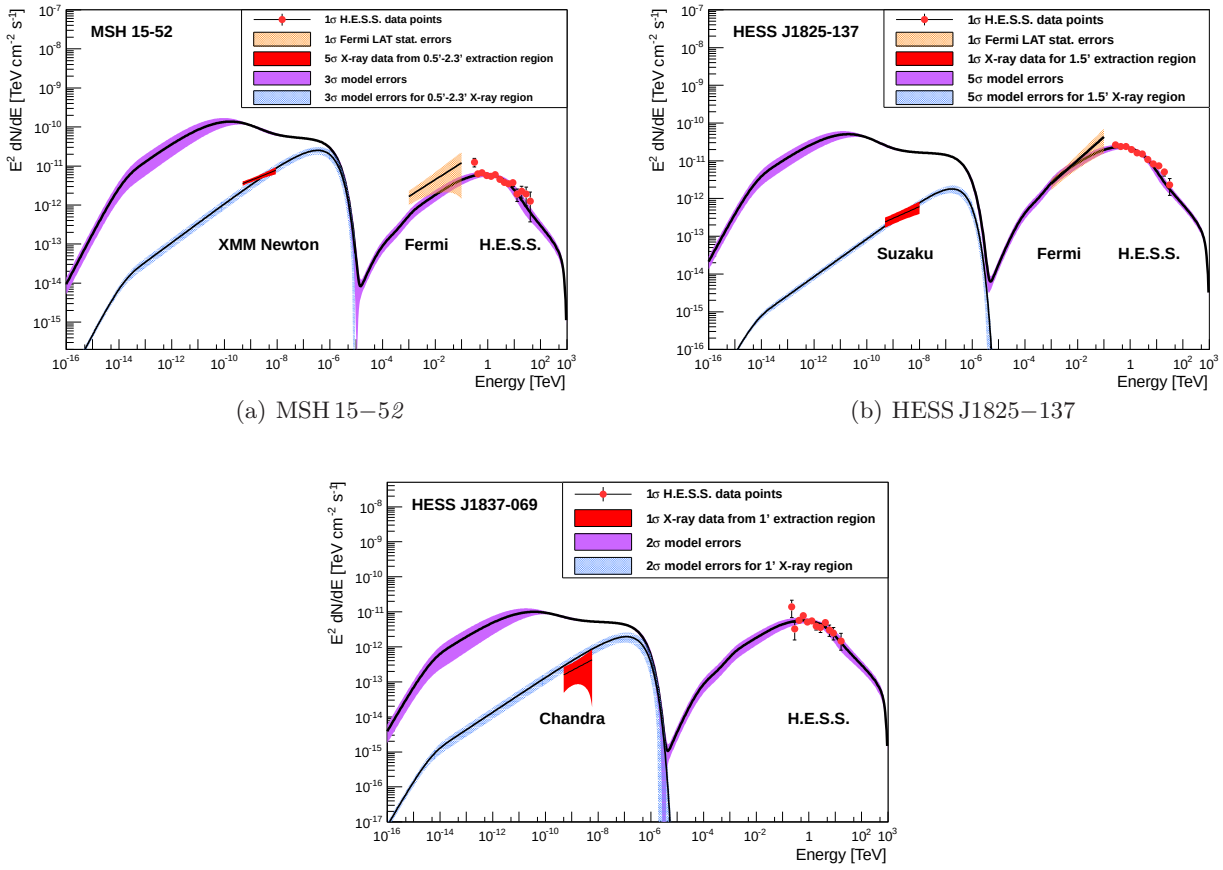
that mainly the youngest leptons account for the X-ray emission while we observe the injection history of the pulsar in VHE γ-rays. This can be understood as the energy of the leptons causing the synchrotron radiation in the considered X-ray regime is higher than the energy of the leptons causing the VHE γ-ray emission via IC scattering (de Jager & Djannati-Ataï, 2009). Numerous highly energetic leptons are present in young populations. For older populations the number of highly energetic leptons has been reduced significantly by cooling processes (mainly synchrotron radiation), which are especially efficient at high energies (see e.g. Blumenthal & Gould, 1970). Thus, for the older populations the synchrotron peak is shifted to lower energies, out of the observational X-ray range.

[1] We neglect a synchrotron self-Compton (SSC) scattering component in the VHE γ-ray spectrum, since this work is focused on evolved pulsars, whereas SSC is relevant mostly for the highly magnetized PWNe of very young and energetic pulsars, e.g. the Crab Nebula (Meyer et al., 2010).

Table 1. Overview of the selected PWNe and their associated pulsars. The list is sorted by increasing characteristic age, representing different evolutionary states. The properties of the pulsars (characteristic age τ_c, current period P, current spin-down luminosity $\dot{E}$ and distance d) are taken from the ATNF pulsar database* (Manchester et al., 2005). References for the H.E.S.S. sources: [1]Aharonian et al. (2005), [2]Aharonian et al. (2006a), [3]Aharonian et al. (2006b).

VHE Source	equiv. VHE source radius [arc min]	Pulsar	τ_c [kyr]	P [ms]	$\dot{E}$ [erg s^{-1}]	d [kpc]
MSH 15−52[1]	11.5	PSR B1509−58	1.55	151	$1.8 \cdot 10^{37}$	5.81
HESS J1825−137[2]	44.0	PSR J1826−1334	21.4	101	$2.8 \cdot 10^{36}$	4.12
HESS J1837−069[3]	13.7	PSR J1837−0604	33.8	96	$2.0 \cdot 10^{36}$	6.19

*URL: `http://www.atnf.csiro.au/research/pulsar/psrcat/`



(a) MSH 15−52 (b) HESS J1825−137

(c) HESS J1837−069

Fig. 3. Spectral energy distributions for the three sources listed in Table 1. The black lines show the modeled SEDs resulting from a fit to the VHE γ-ray data. The violet bands depict the uncertainty of the model based on errors on the fit parameters and their correlations. The blue dotted bands denote the model prediction of the X-ray emission calculated for the published analysis regions (compare Table 4). H.E.S.S. data (red filled circles) are presented along with their $1\,\sigma$ statistical errors. Red filled bands show the X-ray data. Where available we included γ-ray data (orange) from the Fermi Large Area Telescope (Fermi-*LAT*), as well. For better visualization we show higher-level error bands for the X-ray data and for the modeled SEDs. References for the VHE γ-ray and X-ray data can be found in Tables 1 and 4, respectively. Fermi data for MSH 15−52 and for HESS J1825−137 are adopted from Abdo et al. (2010) and Grondin et al. (2011), respectively.

3. Applications

Based on the considerations presented above, evolved PWNe offer a potential explanation for a significant fraction of TeV sources which have remained unidentified up to now. In this scenario, an old pulsar may be surrounded by a relic TeV PWN detectable with current IACTs. However, due to the low present energy output of the pulsar the nebula does not contain enough high-energy leptons to produce a strong X-ray counterpart to the TeV PWN (compare Figs. 1 and 2). This view is in accordance with detailed studies presented, e.g., by de Jager & Djannati-Ataï

Table 2. Application of the model to the selected PWNe. The model was fit to the VHE γ-ray data and the fit results of the free parameters P_0 and B_0 are listed. The interval in parentheses denotes the parameter boundaries during the optimization procedure.

Source	P_0 [ms] $(5-P)$	B_0 [μG] $(5-200)$	χ^2/n.d.f
MSH 15−5*2*	43.5 ± 2.5	85.0 ± 8.3	15.1/12
HESS J1825−137	28.4 ± 0.8	26.9 ± 1.5	30.5/9
HESS J1837−069	39.6 ± 3.7	14.4 ± 3.0	10.0/10

Table 3. Comparison of predicted and measured VHE γ-ray flux for the modeled PWNe. References can be found in the caption of Table 1.

Source	Energy threshold [TeV]	Flux above threshold [10^{-12} cm^{-1} s^{-1}] Model Prediction	Measured
MSH 15−5*2*	> 0.28	19.8 ± 1.1	22.5[a]
HESS J1825−137	> 0.27	73.8 ± 1.8	82.8 ± 2.2
HESS J1837−069	> 0.2	25.2 ± 2.6	30.4 ± 1.6

[a] No statistical errors provided.

Table 4. Comparison of predicted and measured X-ray emission for the modeled PWNe. For each X-ray analysis the published energy range and the radius of the used analysis region are listed. In the case of MSH 15−5*2*, where the authors provide several ring-shaped analysis regions, we combined the innermost three rings in order to use comparable extraction areas for all sources. References to the X-ray data: [1]Schöck et al. (2010), [2]Uchiyama et al. (2009), [3]Gotthelf & Halpern (2008).

Source	Analysis region Radius [arcmin]	Energy range [keV]	F_X^a Model Prediction	F_X^a Measured	Index[b] Model Prediction	Index[b] Measured
MSH 15−5*2*[1]	$0.5-2.3$	$0.5-9$	22.1 ± 2.0	24.9 ± 0.7	1.54 ± 0.04	1.66 ± 0.02[c]
HESS J1825−137[2]	1.5	$0.8-10$	1.82 ± 0.07	1.71 ± 0.47	1.53 ± 0.01	1.69 ± 0.09
HESS J1837−069[3]	1.0	$2-10$	2.5 ± 0.4	1.0[d]	1.57 ± 0.13	1.6 ± 0.4

[a] Energy fluxes are given in units of 10^{-12} erg cm^{-2} s^{-1}.
[b] Photon index of a power-law model.
[c] Photon index from the innermost ring of the X-ray analysis which exhibits the highest energy flux.
[d] No statistical errors provided.

(2009) and Mattana et al. (2009). For some of the unidentified VHE γ-ray sources where an evolved PWN scenario appears likely, deep observations performed with current satellite observatories may yet reveal X-ray counterparts despite the relative weakness of the expected X-ray emission. The model presented in this work allows to select suitable candidates based on an estimate of the required exposure for a detection in the X-ray regime. In order to investigate the reliability of the model we applied it to three selected PWNe, which are listed in Table 1. The motivation for this selection was to sample PWNe from different states of evolution for which both VHE γ-ray and X-ray spectra of sufficient quality are available. Since the model is radially symmetric it was necessary to define a circular source area as an approximation to the asymmetrical Gaussian morphology fits of the published VHE γ-ray data. The radius was chosen such that the circle covers an area equivalent to the $3\,\sigma$ extent of the ellipse obtained from the VHE morphology fits. The values of the equivalent radii are included in Table 1.

Having calculated the equivalent circular extent of the VHE γ-ray source the free parameters of the model were fixed by a χ^2 fit to the VHE γ-ray data using the MINUIT minimization package (James & Roos, 1975). Note that only statistical errors ($1\,\sigma$) of the VHE γ-ray data are taken into account. The optimized parameters and the predictions of the VHE γ-ray fluxes are presented in Tables 2 and 3. The modeled SEDs are confronted with observational X-ray, γ-ray (where available) and VHE γ-ray data in Fig. 3. In the VHE γ-ray range spectral points were available, while in X-rays and γ-rays the shown bands correspond to the published power-law fit with the parameters (index and normalization or energy flux) assumed to be uncorrelated. The confidence bands of the fitted model were calculated using Gaussian error propagation and take the errors of the fit parameters as well as their correlations into account. The level of the quoted error bands is adapted individually for the different sources for reasons of enhanced visibility (see caption of Fig. 3).

The comparison shows that the γ-ray and VHE γ-ray data are reasonably well described by the model (violet bands), whereas the X-ray data are strongly overestimated.

However, this is expected since the extraction region for the spectrum determination is usually much smaller in X-rays than in VHE γ-rays. The resulting mismatch between the lepton population used for the modeling and the one observed in X-rays has to be taken into account. In the following, we use the relation between the spatial extent of the lepton population and their age, given in Eq. 11: Starting from the given size of the X-ray spectrum extraction region we determine the corresponding maximum age $t_{\mathrm{lept.,\,max}}$ of the leptons producing the emission. In the next step, we re-calculate the amount and energy distribution of the leptons contained within this region[2] by using $T - t_{\mathrm{lept.,\,max}}$ as a starting point for the evaluation of Eq. 13. The resulting modified SEDs with their corresponding uncertainties, shown as blue dotted bands in Fig. 3, are clearly in better agreement with the observational data. A quantitative comparison between modeled and measured values of the X-ray flux is given in Table 4.

Our study indicates that, with the above introduced adaption of the spatial extent of the lepton population responsible for the observed X-ray emission, the presented time-dependent model allows to reproduce the broad-band non-thermal emission of PWNe of different evolutionary states. Hence, transferring the model to yet unidentified VHE γ-ray sources which are considered candidates for middle-aged PWNe, the predictions of the X-ray flux can help to evaluate whether deep X-ray observations with current satellites may be beneficial for a firm identification of the nature of such sources.

4. Conclusions

Motivated by the large number of yet unidentified VHE γ-ray sources suspected to be evolved PWNe, we developed a time-dependent leptonic model suitable to calculate the non-thermal emission from PWNe of different ages. The presented model allows to study the expected photon SEDs evolving with the age of the PWN. Our study yields additional support for the conception that evolved PWNe are still bright in VHE γ-rays, while their X-ray emission is largely suppressed and hence difficult to detect.

Moreover, in this work we investigate the contribution of leptons of different epochs to the current photon SED in detail. In particular for older PWNe it is necessary to take into account the time dependence of lepton injection and cooling effects in order to explain the observed VHE γ-ray emission, whereas the X-ray emission (especially in the vicinity of the pulsar) is dominated by the young lepton population.

Finally, we tested whether our model can be used to predict the X-ray flux of an unidentified source based on the VHE γ-ray detection. We selected three representative PWNe of different evolutionary states and fixed the free parameters of the model by a fit to observational VHE γ-ray data. The comparison of modeling results and observational data shows that the emission in the high-energy range can be predicted successfully.

Acknowledgements. The authors wish to acknowledge the helpful comments by members of the H.E.S.S. collaboration. Moreover, we thank Peter Eger and Markus Holler for the fruitful discussions concerning X-ray observations and their analysis.

[2] In a full three-dimensional treatment it would be necessary to consider also older leptons (with ages $t_{\mathrm{lept.}} > t_{\mathrm{lept.,\,max}}$) that are located along the line of sight. However, their contribution to the X-ray emission is supposed to be small and hence neglected.

References

Abdo, A. A., Ackermann, M., Ajello, M., et al. 2010, ApJ, 714, 927
Aharonian, F., Akhperjanian, A. G., Aye, K.-M., et al. 2005, A&A, 435, L17
Aharonian, F., Akhperjanian, A. G., Barres de Almeida, U., et al. 2008, A&A, 477, 353
Aharonian, F., Akhperjanian, A. G., Bazer-Bachi, A. R., et al. 2006a, A&A, 460, 365
Aharonian, F., Akhperjanian, A. G., Bazer-Bachi, A. R., et al. 2006b, ApJ, 636, 777
Blondin, J. M., Chevalier, R. A., & Frierson, D. M. 2001, ApJ, 563, 806
Blumenthal, G. R. & Gould, R. J. 1970, Rev. Mod. Phys., 42, 237
Camilo, F., Kaspi, V. M., Lyne, A. G., et al. 2000, ApJ, 541, 367
de Jager, O. C. & Djannati-Ataï, A. 2009, in Astrophysics and Space Science Library, Vol. 357, Astrophysics and Space Science Library, ed. W. Becker, 451
Gaensler, B. M. & Slane, P. O. 2006, ARA&A, 44, 17
Gelfand, J. D., Slane, P. O., & Zhang, W. 2009, ApJ, 703, 2051
Gotthelf, E. V. & Halpern, J. P. 2008, ApJ, 681, 515
Grondin, M.-H., Funk, S., Lemoine-Goumard, M., et al. 2011, ApJ, 738, 42
James, F. & Roos, M. 1975, Computer Physics Communications, 10, 343
Livingstone, M. A., Kaspi, V. M., Gavriil, F. P., & Manchester, R. N. 2005, The Astrophysical Journal, 619, 1046
Manchester, R. N., Hobbs, G. B., Teoh, A., & Hobbs, M. 2005, VizieR Online Data Catalog, 7245, 0
Manchester, R. N. & Taylor, J. H. 1977, Pulsars., ed. Smith, F. G.
Mattana, F., Falanga, M., Götz, D., et al. 2009, ApJ, 694, 12
Meyer, M., Horns, D., & Zechlin, H.-S. 2010, A&A, 523, A2+
Pacini, F. & Salvati, M. 1973, ApJ, 186, 249
Porter, T. A. & Strong, A. W. 2005, in International Cosmic Ray Conference, Vol. 4, International Cosmic Ray Conference, 77
Qiao, W.-F., Zhang, L., & Fang, J. 2009, Research in Astronomy and Astrophysics, 9, 449
Schöck, F. M., Büsching, I., de Jager, O. C., Eger, P., & Vorster, M. J. 2010, A&A, 515, A109+
Uchiyama, H., Matsumoto, H., Tsuru, T. G., Koyama, K., & Bamba, A. 2009, PASJ, 61, 189
van der Swaluw, E., Downes, T. P., & Keegan, R. 2004, A&A, 420, 937
Zhang, L., Chen, S. B., & Fang, J. 2008, ApJ, 676, 1210